Electrostatic and Nonpolar Peptide–Membrane Interactions. Lipid Binding and Functional Properties of Somatostatin Analogues of Charge $z = +1$ to $z = +3$†

Joachim Seelig,*,‡ Simon Nebel,‡ Peter Ganz,‡ and Christian Bruns§

Department of Biophysical Chemistry, Biocenter of the University of Basel, Klingelbergstrasse 70, CH-4056 Basel, Switzerland, and SANDOZ-Pharma Ltd., CH-4002 Basel, Switzerland

Received April 7, 1993; Revised Manuscript Received June 8, 1993

ABSTRACT: The interaction of four structurally related somatostatin analogues (effective electric charge $+0.4 \leq z \leq +3$) with lipid membranes was studied with titration calorimetry and was compared with the functional activity of the peptides. Surface activity measurements provided average cross-sections of 70 or 135 Å^2, indicating that the cyclic molecules orient at the air–water interface with their ring system either parallel ($z = +3$) or perpendicular ($z = +1$) to the surface or switching between the two orientations according to the surface density ($z = +2$). The nonspecific binding of the peptides to sonified lipid vesicles was enthalpy-driven with a ΔH of –4 to –7.5 kcal/mol. A consistent quantitative analysis of the binding isotherms was achieved by combining electrostatic attractions, calculated via the Gouy–Chapman theory, with a nonspecific surface partition equilibrium for the nonpolar interactions. The electrostatic attraction of the cationic peptides varied strongly according to the peptide charge. Due to the flat ring structure of the cyclic peptides, their true physical charge was sensed at the membrane surface, and no "charge screening" was observed. Peptide binding to the negative charged membrane was accompanied by a proton-uptake of the N-terminal amino group of 0.23–0.38 H^+/peptide. Deviations from the theoretical prediction of 0.39 H^+/peptide can be explained by a preferential binding of the nonprotonated species. The nonpolar interactions, as described by the surface partition coefficients of the four peptides, fell into a narrow range of $K \simeq 50$–230 M^{-1} whereas the apparent overall binding constants were between 200 and 5000 M^{-1}. The binding affinities to the somatostatin receptors varied considerably with dissociation constants from 2.8×10^{-10} to 3×10^{-6} M and paralleled the inhibitory effect of the peptides on growth hormone release. Functional activity appeared to correlate inversely with lipid binding, suggesting that those peptides which were bound too tightly to the lipid phase had a decreased probability to react with the active site on the protein receptor.

Somatostatin, the growth-hormone release inhibiting factor, is also a potent inhibitor for the release of a number of other bioactive molecules such as glucagon, gastrin, insulin, etc. Many different somatostatin derivatives have been synthesized in order to test their potential for clinical application. In particular, the octapeptide SMS 201–995 (octreotide, Sandostatin)[1] was found to have an even greater biological activity than somatostatin itself (Maurer et al., 1982). The side chain sequence Phe^3-D-Trp^4-Lys^5-Thr^6 of SMS 201–995 also occurs in somatostatin (with L-Trp^4) and appears to be a key element for receptor binding which is highly specific with a dissociation constant of $K_D = 0.3$ nM. Somatostatin and its analogue SMS 201–995 also bind to pure lipid membranes, albeit with much smaller binding constants (Beschiaschvili & Seelig, 1990, 1992).[2] Nevertheless, binding to the membrane will compete with receptor binding because of the large excess of membrane surface over receptor sites. Partitioning into the lipid phase could be disadvantageous since (i) peptide is lost from the aqueous phase and is not available for receptor binding if the binding site is in an extracellular loop and (ii) unfavorable side effects due to the perturbation of the membrane structure might occur. On the other hand, if the active site of the receptor is located in the hydrophobic part of the bilayer, membrane binding can be advantageous because (i) it may induce the pharmacologically active conformation (Schwyzer, 1987) and (ii) it restricts the motion of the peptide to a two-dimensional diffusion which is distinctly faster than bulk diffusion (Rhodes et al., 1985; Herbette et al., 1991). In evaluating the various possibilities, it must be borne in mind that lipid–peptide interactions can be purely electrostatic (attraction of a cationic peptide to a negatively charged membrane *surface*), purely hydrophobic (absorption of a highly lipophilic peptide into the membrane *interior*), or a combination of both.

In the present study we compare the lipid-binding properties of four chemically related but electrically different somatostatin analogues, the chemical structures and maximum charges of which are summarized below. The cyclic octapeptide SMS 201–995 carries a maximum electric charge of $z = +2$ if the N-terminal amino group is fully protonated. However, at pH 7.4 the effective charge is only $\langle z \rangle = 1.4$. The molecule has approximate dimensions of $20 \times 7 \times 7$ Å^3 and binds to phospholipid membranes with the plane of the peptide ring parallel to the membrane surface (Beschiaschvili & Seelig, 1990). Upon binding, the peptide intercalates between the

† This work was supported in part by the Swiss National Science Foundation (Grant 3100-27505.89).

‡ Biocenter of the University of Basel.

§ SANDOZ-Pharma Ltd.

[1] Abbreviations: PC, phosphatidylcholine; PG, phosphatidylglycerol; POPC, 1-palmitoyl-2-oleoyl-*sn*-glycero-3-phosphocholine; POPG, 1-palmitoyl-2-oleoyl-*sn*-glycero-3-phosphoglycerol; SMS 201-995, D-Phe^1-Cys^2-Phe^3-D-Trp^4-Lys^5-Thr^6-Cys^7-Thr^8-(ol) = (octreotide, Sandostatin); SDZ 206–276, L-Phe^1-octreotide; SDS 214–324, Lys^0-octreotide; SDS 217–717, citrullin^5-octreotide.

[2] The term *membrane binding* has two different meanings in the present context. On the one hand it describes the nonspecific peptide–lipid interaction, composed of an electrostatic adsorption to the membrane surface followed by a partitioning into the membrane interior; on the other hand it refers to the highly specific binding of the peptides to the active site on the membrane-bound receptor molecule. In the case of ambiguities, we shall use the synonym *adsorption/partitioning* for the former process.

0006-2960/93/0432-9714$04.00/0

lipid molecules, and its electric charge induces a reorientation of the phosphocholine dipoles. Using ^2H NMR spectroscopy, it could be demonstrated that the positive end of the P–N dipole moves toward the water phase (Beschiavili & Seelig, 1991).

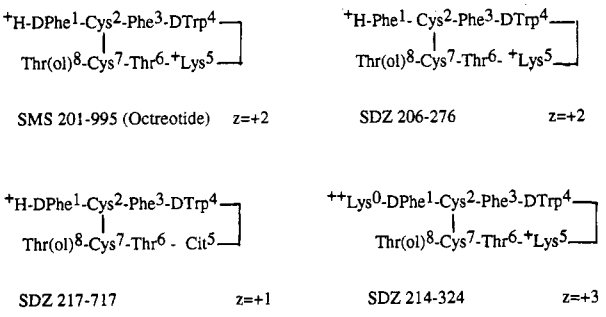

Electrostatic as well as nonpolar interactions contribute to the bilayer binding of peptide SMS 201–995. The peptide concentration at the bilayer–water interface, C_I, depends strongly on the electric surface charge density of the membrane and can be accounted for quantitatively by using the Gouy–Chapman theory [for general reviews of this theory see Aveyard and Haydon (1973) and McLaughlin (1977, 1989); its specific application to the binding of peptide SMS 201–995 is discussed in Beschiaschvili and Seelig (1990, 1992)]. Following electrostatic attraction, the second step in the binding process is the transition of the peptide from the aqueous interface (with increased peptide concentration, C_I) to the plane of binding on the membrane. Using the surface concentration, C_I, the "chemical" binding step of peptide SMS 201–995 can be described by a simple surface partition equilibrium with a surface partition coefficient (intrinsic binding constant) of $K \sim 70\ M^{-1}$.

For the somatostatin analogue SMS 201–995, the binding equilibrium was studied by four different techniques (monolayer expansion method, ultracentrifugation assay, ζ-potential measurement, and high-sensitivity titration calorimetry) leading to a consistent picture of the binding mechanism and the binding parameters. Titration calorimetry was particularly useful in this respect since it allowed the evaluation not only of the binding enthalpy but also of the binding constant. Surprisingly, the binding of compound SMS 201–995 was found to be enthalpy-driven for small, sonicated lipid vesicles but entropy-driven for planar membranes (Beschiaschvili & Seelig, 1992). In addition, the measurements revealed a pK-shift of the N-terminal amino group: binding of SMS 201–995 to neutral membranes decreased the pK of the NH_3^+ group; binding to negatively charged membranes increased it.

In the present study we have extended this peptide–lipid binding model experimentally and theoretically by the following modification. (i) In peptides SDZ 217–717 and SDZ 214–324, the maximum electric charge is decreased or increased by one unit, i.e., to $z = +1$ or $z = +3$, respectively. This is achieved by replacing Lys^5 with the noncharged amino acid citrullin (SDZ 217–717) or by adding an additional lysin at the N-terminus (SDZ 214–324). These substitutions have distinct consequences on the electrostatic attraction and, in turn, on the surface concentrations of the two peptides. (ii) A purely structural modification is introduced in compound SDZ 206–276 where D-Phe^1 of peptide SMS 201–995 is replaced by L-Phe^1. Inspection of molecular models reveals that this substitution aligns three aromatic residues on the same side of the peptide ring. Electrostatic effects being unchanged ($z = +2$ for both molecules), the "chemical" contribution to the binding process can be expected to increase due to the more hydrophobic face of peptide SDZ 206–276. (iii) The binding model is refined by including a pH regulation of the effective peptide charge. In the case of a negatively charged membrane not only the cationic peptide but also all other cations will accumulate at the lipid–water interface. In particular, the pH near the plane of binding will be more acidic than in bulk solution (Fernandez & Fromherz, 1977; Fromherz, 1989; Miyazaki et al., 1992; Cevc & Marsh, 1987). Since the pK of the N-terminal amino group is $\sim$7.2, any variation in pH influences the electric charge of the peptide (Seelig, 1990). The refined model takes into account the increase in the effective charge of the peptide as it approaches the lipid–water interface, whereas the previous analysis was based on a fixed average charge. (iv) The electric charge not only influences the electrostatic attraction but also may affect the chemical binding step. If pH $\sim$ pK, two peptide species with charges z and $z + 1$ will accumulate at the lipid–water interface. We investigate the possibility that the two species have different binding constants and demonstrate that binding studies in buffers of different dissociation enthalpies allow a determination of the two parameters. (v) Finally, we compare the nonspecific binding to the lipid membrane with the specific binding to the somatostatin receptors and with the functional activities of the analogues in inhibiting the growth hormone release from pituitary cells. This sheds light on the question of how the interaction of the peptides with the lipid phase interferes with their biological activities.

MATERIALS AND METHODS

Materials. The peptide analogues shown above were kindly provided by SANDOZ-Pharma AG (Basel, Switzerland) and had a purity of better than 95%. The peptide concentrations were determined with UV spectroscopy using an absorption coefficient of $\epsilon = 5700\ M^{-1}\ cm^{-1}$ ($\lambda = 280$ nm) (Holladay et al., 1977). 1-Palmitoyl-2-oleoyl-*sn*-glycero-3-phosphocholine (POPC) and 1-palmitoyl-2-oleoyl-*sn*-glycero-3-phosphoglycerol (POPG) were purchased from Avanti Polar Lipids (Birmingham, AL). All other chemicals were purchased at highest purity from commercial sources.

Surface Activity Measurements. The monolayer apparatus consisted of a round Teflon trough designed by Fromherz (1975) with a total area of 362 cm^2 divided into eight compartments. The surface pressure was measured by the Wilhelmy Method using plates cut from filter paper (Whatman, No. 1). Peptides were dissolved in distilled water, yielding clear solutions. Small amounts of the peptide stock solution, freshly prepared before use, were then injected into the buffer, and the increase of the surface tension was monitored until equilibrium was reached. Measurements were made at room temperature.

Preparation of Lipid Vesicles. Small unilamellar vesicles of diameter $\sim$30 nm were prepared as follows. The lipids were dissolved in dichloromethane, mixed in the desired ratio, and dried overnight under high vacuum. Buffer (100 mM NaCl plus 10 mM Tris, MOPS, or phosphate) was added to the dry film, and the suspension was vortexed extensively. Next, the lipid dispersions were sonified under a nitrogen atmosphere for 35–45 min (at 10 °C) until an almost clear solution was obtained. Metal debris from the titanium tip was removed by centrifugation in an Eppendorf centrifuge for 10 min.

Titration Calorimetry. Isothermal titration calorimetry was performed using an Omega MC-2 instrument from

Micrococal (Microcal, Northhampton, MA) (Wiseman et al., 1989). All experiments were done at 28 °C. Solutions were degassed under vacuum prior to use. The calorimeter was calibrated electrically. Briefly, phospholipids were injected in 10-μL increments into a solution of peptide (cell volume = 1.2778 mL) dissolved in the same buffer as the lipid vesicles. Control experiments were performed by making identical injections of lipid vesicles into a cell containing buffer with no peptide. The starting solutions in the calorimeter cell and in the injection syringe were at the same temperature. For those peptides which exhibited a sufficiently strong binding to the lipid vesicles, the reverse experiment was also performed: the calorimeter cell was filled with buffer containing small unilamellar vesicles, and a peptide solution was injected in 10-μL steps. Under conditions of complete peptide binding, each injection step provides the complete heat of reaction.

Radioligand Binding Studies. The binding studies were performed using [^{125}I]Tyr^3-octreotide (SDZ 204–090), a well-characterized ligand for somatostatin receptors (Bruns et al., 1990). SDZ 204–090 was iodinated by the chloramine T method (specific radioactivity: 2000 Ci/mmol). The binding assay was performed in 10 mM HEPES buffer as described previously (Reubi et al., 1981). Briefly, rat cortical membranes (50 μg of protein/tube) were incubated in a total volume of 300 μL at room temperature for 30 min with approximately 25 pmol/L of radioligand and increasing concentrations of unlabeled peptide. The incubation was terminated by rapid filtration through Whatman GF/C filters. Filters were washed with 20 mL of ice-cold Tris buffer (10 mM, pH 7.5), and the radioactivity was counted in an LKB gamma counter. All experiments were performed in triplicate. The binding data were analyzed according to a one-site model using the nonlinear regression computer program SCTFIT developed by de Lean (1979).

Growth Hormone Release. Pituitary glands were removed from rats (Iffa Credo, Lyon, France) with a mean body weight of 200 g. The pituitary cells were prepared as previously described (Vale & Grant, 1975). They were cultured for 4 days in minimum essential medium, supplemented with 5% fetal calf serum, 5% horse serum, 43 mmol/L $NaHCO_3$, 100 ng/L streptomycin, and 10^{-5} units/L penicillin. The somatostatin analogues were administered in the presence of D-Ala^2-GHRH(1–29)amide (3×10^{-10} mol/L) for 3 h. Growth hormone in the supernatant was determined by means of radioimmunoassay.

RESULTS

Surface Activity Measurements. The surface activities of peptides SMS 201–995, SDZ 217–717, and SDZ 214–324 were measured in buffer at pH 7.4 as a function of the peptide concentration, and the results are summarized in Figure 1. The citrullin derivative SDZ 217–717, which carries the smallest electric charge ($\langle z \rangle = 0.4$ at pH 7.4) exhibits the strongest surface activity and the lysine derivative SDZ 214–324, with $\langle z \rangle = 2.4$, the smallest surface activity. Peptide SMS 201–995 ($\langle z \rangle = 1.4$) falls between the two extremes. From the slopes of these *Gibbs adsorption isotherms*, it is possible to determine the excess concentration Γ of solute at the surface according to

$$\Gamma = (1/RT)(\partial\pi/\partial \ln c) \qquad (1)$$

with R = gas constant, T = absolute temperature, π = surface pressure, and c = concentration of peptide in solution. Γ is

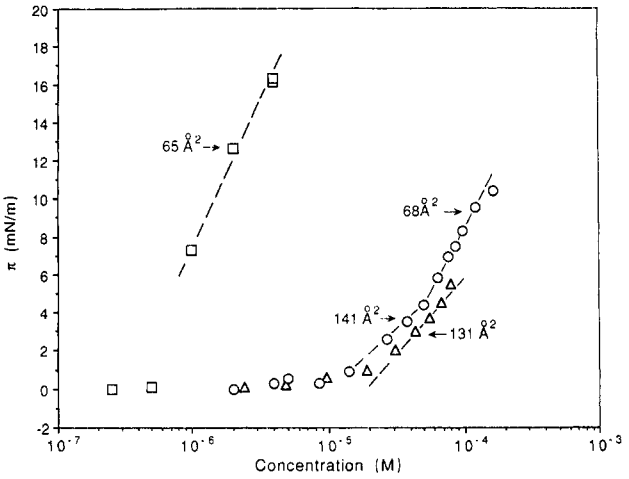

FIGURE 1: Surface pressure π as a function of the peptide concentration (logarithmic scale) for the different somatostatin analogues. (○) Peptide SMS 201–995 with $\langle z \rangle = 1.4$; (□) peptide SDZ 217–717 with $\langle z \rangle = 0.4$; (△) peptide SDZ 214–324 with $\langle z \rangle = +2.4$. Measurements were in buffer (0.1 M NaCl + 10 mM Tris) at pH 7.4 and 22 °C.

related to the surface area requirement, A_P, of the individual peptide molecule according to

$$A_P = 1/(\Gamma N_A) \qquad (2)$$

with N_A = Avogadro's number. Evaluation of Figure 1 yields surface areas of $A_P \simeq 65$ Å^2 for peptide SDZ 217–717 ($\langle z \rangle = 0.4$) and $A_P \simeq 131$ Å^2 for peptide SDZ 214–324 ($\langle z \rangle = 2.4$). Peptide SMS 201–995 ($\langle z \rangle = 1.4$) exhibits a biphasic behavior with a surface area of $A_P \simeq 141$ Å^2 at low peptide concentration, and hence low surface density, and $A_P \simeq 68$ Å^2 at high packing density. Inspection of molecular models reveals a surface area of the $\sim 7 \times 20 = 140$ Å^2 and a cross-sectional area of $\sim 7 \times 7 = 49$ Å^2 for the cyclic peptides. Comparison with the experimental data suggests that peptide SDZ 214–324 aligns with the plane of its ring system parallel to the water surface, peptide SDZ 217–717 aligns perpendicular to the surface, and peptide SMS 201–995 switches from a parallel to a perpendicular orientation as the packing density at the air–water interface increases.

Calorimetric Titrations. Two sets of raw data, the titration of peptides SDZ 217–717 ($\langle z \rangle = 0.4$ at pH 7.4) and SDZ 214–324 ($\langle z \rangle = 2.4$ at pH 7.4), with negatively charged POPC/POPG (75/25 mol/mol) vesicles are shown in Figure 2. After each injection of lipid vesicles, the binding/adsorption of peptide to the outer membrane surface produces an exothermic heat effect. With increasing numbers of injections, the magnitude of the measured reaction enthalpy gradually decreases. For peptide SDZ 214–324 with its large positive charge of $\langle z \rangle = 2.4$, this effect is more pronounced than for peptide SDZ 217–717 with $\langle z \rangle = 0.4$. Control experiments, in which the same lipid vesicles were injected into buffer without protein, showed only small exothermic heats of reaction (−1 to −3 μcal) which were subtracted in the final analysis.

The calorimetric binding enthalpy was obtained by integrating the area under each peak. Figure 3A then summarizes the variation of the cumulative heat of reaction with the number of injections for SDZ 214–324. The solid line in Figure 3A was calculated by combining the electrostatic attraction (calculated with the Gouy–Chapman theory) with a surface partition equilibrium (cf. below). The quantitative analysis allows the evaluation of both the reaction enthalpy and the corresponding binding constant yielding $\Delta H = -6.5$ kcal/mol

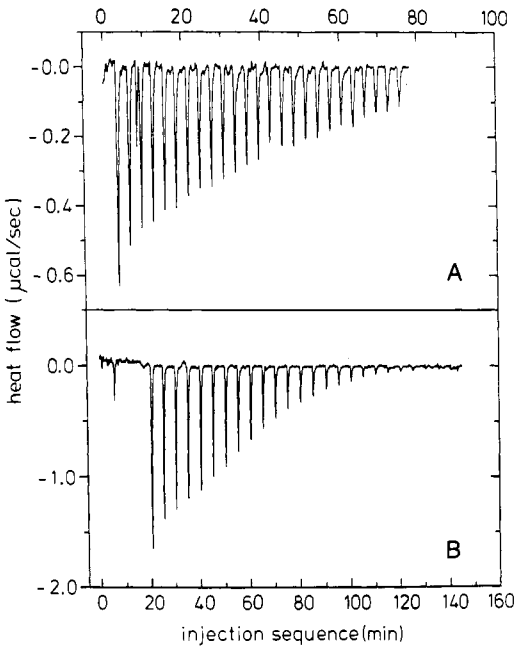

FIGURE 2: Titration calorimetry of peptide solutions with small unilamellar lipid vesicles. Influence of peptide charge. (A) Peptide SDZ 217–717 (129 μM), dissolved in buffer (0.1 M NaCl, 10 mM Tris, pH 7.4). Average charge in buffer $\langle z \rangle$ = 0.4. Each peak corresponds to the injection of 10 μL of sonified phospholipid vesicles (POPC/POPG; 75/25 mol/mol) dispersed in the same buffer. The total lipid concentration was 33.5 mM, but only the outside of the lipid vesicles (20.1 mM) was available for peptide binding. Measurement was at 28 °C. (B) Peptide SDZ 214–324 (70.4 μM) with $\langle z \rangle$ = 2.4 dissolved in the same buffer as in panel A. Injection of POPC/POPG (75/25 mol/mol) vesicles was in 10-μL steps. Total lipid concentration was 44.2 mM. Lipid concentration available for binding was 26.5 mM. Temperature, 28 °C.

and K = 50 M^{-1} for peptide SDZ 214–324 ($\langle z \rangle$ = 2.4). The same analysis applied to peptide SDZ 217–717 ($\langle z \rangle$ = 0.4, data of Figure 2A) leads to ΔH = –4.0 kcal/mol and $K \approx 80$ M^{-1}. The difference in the appearance of the titration curves shown in Figure 2 is thus caused by the larger electrostatic attraction experienced by peptide SDZ 214–324 ($\langle z \rangle$ = 2.4) and not so much by differences in ΔH or K.

Titration experiments were performed in three different buffers and at two different pH values (pH 6.25 and 7.4). The data are summarized in Table I. At pH 6.25 the terminal amino group is fully protonated, and the peptides carry their respective maximum charge; at pH 7.4 only 40% of the terminal amino groups are charged (p$K \sim 7.2$), and the peptides become further protonated as they approach the more acidic membrane surface. This is demonstrated experimentally by plotting the measured reaction enthalpy versus the buffer dissociation enthalpy, as shown for peptide SDZ 206–276 and SDZ 217–717 (Figures 4 and 5, respectively).

At pH 6.25 the measured reaction enthalpy is independent of the type of buffer employed. In contrast, at pH 7.4 a linear variation of the measured ΔH with the buffer dissociation enthalpy ΔH_{Diss} is observed with

$$\Delta H = -6.9 + 0.23\ \Delta H_{Diss}\ (\text{kcal/mol}) \qquad (3a)$$

for peptide SDZ 206–276 and

$$\Delta H = -7.8 + 0.34\ \Delta H_{Diss}\ (\text{kcal/mol}) \qquad (3b)$$

for peptide SDZ 217–717. A similar relationship with a slope of n = 0.38 has been reported previously for peptide SMS 201–995 (Beschiaschvili & Seelig, 1992).

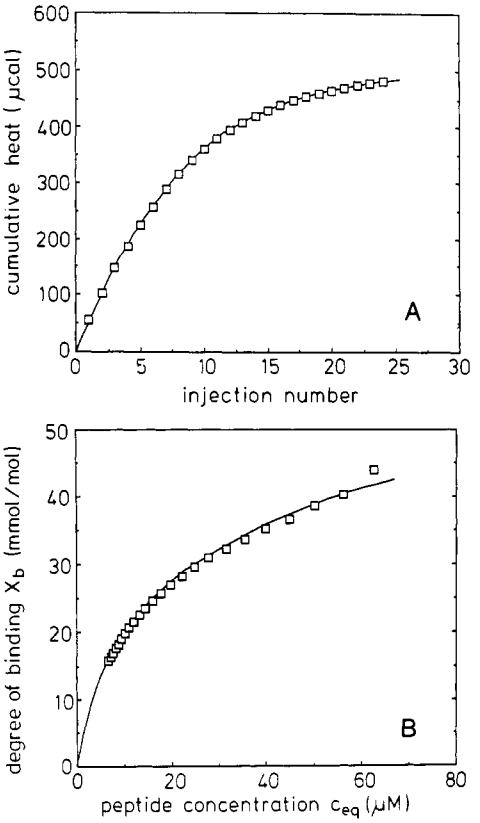

FIGURE 3: Comparison of experimental binding data with the predictions of the Gouy–Chapman theory combined with a surface partition equilibrium. Experimental data for peptide SDZ 214–324 were taken from Figure 2B. The solid lines were calculated with K = 44 M^{-1}, ΔH = –5.9 kcal/mol, z = 2, and pK = 7.2. The effective peptide charge increases from $\langle z \rangle$ = 2.4 in buffer to $\langle z \rangle \simeq 2.75$ at the membrane surface. (A) Cumulative reaction enthalpy as a function of the number of injections. (B) Degree of binding, X_b (mmoles peptide bound per mole total lipid), as a function of peptide concentration. The amount of bound peptide after "i" injection steps is proportional to $\sum_i \Delta h_i / \Delta H$, which can be translated into X_b and C_{eq}. While panel B provides a more direct physical insight, the simulation of the primary experimental data (Figure 2A) yields a better accuracy. The cumulative heat $\sum \Delta h_i$ changes by a factor of 10, X_b only by a factor of 2–3.

Functional Assays. The inhibitory effect of the somatostatin analogs on the (GHRH)-induced growth hormone release was determined using a 4-day primary culture of rat anterior pituitary cells. SMS 201–995 and the Lys^0-analogue (SDZ 214–324) were the most effective peptides tested in this series of somatostatin analogues with inhibitory effects of IC_{50} = 1.3×10^{-9} mol/L and 1.2×10^{-9} mol/L, respectively. SDZ 206–276 (L-Phe^1-octreotide) was less active. An inhibitory effect of $IC_{50} = 7.6 \times 10^{-9}$ was determined. In contrast, SDZ 217–717 (5-L-citrullin-octreotide) was nearly ineffective (IC_{50} = 3×10^{-6} mol/L). In addition, binding studies were performed with rat cortical membranes, using [^{125}I]Tyr^3-octreotide as a specific radioligand. Again, SMS 201–995 and SDZ 214–324 were very active in displacing the radioligand from its high-affinity binding site ($IC_{50} = 4.6 \times 10^{-10}$ mol/L and $IC_{50} = 2.8 \times 10^{-10}$ mol/L, respectively). SDZ 206–276 showed a lower binding affinity for somatostatin receptors ($IC_{50} = 2.4 \times 10^{-9}$ mol/L) which parallels the lower potency of this analogue to inhibit growth hormone release. SDZ 217–717 exhibited only a very weak affinity (IC_{50} = 3×10^{-6} mol/L). Table II summarizes the binding affinities and in vitro activities and also provides relative values as referred to SMS 201–995.

Table I: Thermodynamic Parameters of Somatostatin Analogues as Derived from Calorimetric Titration of Small Unilamellar Lipid Vesicles (POPC/POPG, 75/25 mol/mol) T = 28 °C

peptide	peptide conc (μM)	pH	buffer, 0.1 M NaCl plus	peptide charge $\langle z \rangle$ bulk solution	peptide charge $\langle z \rangle$ membrane	K (M^{-1})	ΔG (kcal/mol)	ΔH (kcal/mol)
SMS 201–995[a] (D-Phe[1])	70–110	7.4	10 mM Tris	1.39	1.78–1.74	65 ± 15[b]	−4.8 ± 0.2[c]	−6.3 ± 0.2[b]
	46	7.4	10 mM PO_4^-	1.39	1.78–1.74	60	−4.8	−12.5
	50	6.25	10 mM PO_4^-	1.90	1.98	90	−5.0	−7.3
SDZ 206–276 (L-Phe[1])	73.9	7.4	10 mM Tris	1.39	1.77–1.65	190	−5.5	−4.3
	87.5	7.4	10 mM Tris	1.39	1.76–1.63	190		−4.3
	92.6	7.4	10 mM MPOS	1.39	1.75–1.62	220	−5.6	−5.7
	63.7	7.4	10 mM MOPS	1.39	1.78–1.68	220		−5.4
	61.05	7.4	10 mM PO_4^-	1.39	1.77–1.63	260	−5.7	−6.6
	61.05	7.4	10 mM PO_4^-	1.93	1.77–1.63	260		−6.8
	87.9	6.25	10 mM PO_4^-	1.90	1.98–1.95	260		−4.7
	71.4	6.25	10 mM MOPS	1.90	1.98–1.95	200	−5.5	−4.7
SDZ 217–717 (Cit[5])	129	7.4	10 mM Tris	0.39	0.78–0.6	75	−4.9	−4.0
	97	7.4	10 mM MOPS	0.39	0.79	75		−6.2
	119	7.4	10 mM PO_4^-	0.39	0.78	75		−7.5
	139	6.25	10 mM MOPS	0.9	0.98	90	−5.0	−4.5
	106	6.25	10 mM PO_4^-	0.9	0.98	90		−5.1
	162	6.25	10 mM PO_4^-	0.9	0.98	90		−4.6
SDZ 214–324 (Lys[0])	50	7.4	10 mM Tris	2.39	2.75–2.67	50	−4.7	−6.5

[a] Data were taken, in part, from Beschiaschvili and Seelig (1992), Table III, plus additional measurements. Previous data were reevaluated with the new model. [b] Average of four measurements. [c] Calculated according to $\Delta G = -RT \ln(55.5K)$ where the factor 55.5 takes into account the cratic contribution (Cantor & Schimmel, 1980).

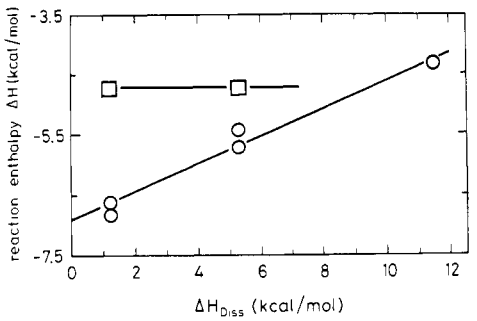

FIGURE 4: Variation of the binding enthalpy of peptide SDZ 206–276 with the buffer dissociation enthalpy. Measurements were made in Tris (ΔH_{Diss} = 11.51 kcal/mol), MOPS (ΔH_{Diss} = 5.29 kcal/mol), and phosphate buffer (ΔH_{Diss} = 1.22 kcal/mol) (Morin & Freire, 1991). Buffer composition: 0.1 M NaCl plus 10 mM Tris, 10 mM MOPS, or 10 mM phosphate. (□) Measurements at pH 6.25; (○) measurements at pH 7.4. Binding measured with sonified unilamellar vesicles composed of POPC/POPG (75/25 mol/mol).

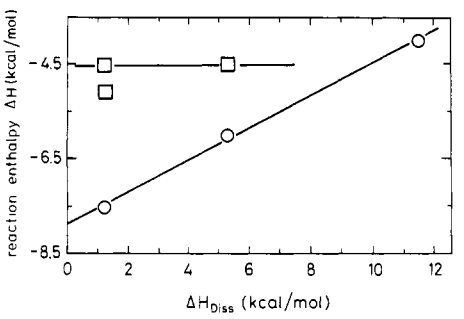

FIGURE 5: Variation of the peptide binding enthalpy of peptide SDZ 217–717 with the buffer dissociation enthalpy. Same buffers as in Figure 4. (□) Measurements at pH 6.25; (○) measurements at pH 7.4.

DISCUSSION

The Binding Model. The peptide binding model is summarized by the following scheme:

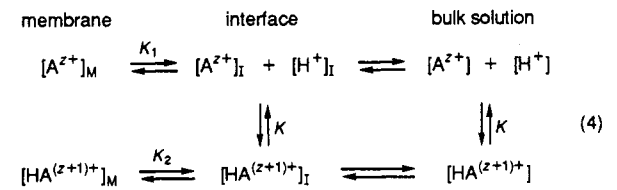

(4)

Three separate regions are distinguished: (i) the bulk solution, (ii) the aqueous layer immediately above the plane of binding (interface "I"), and (iii) the membrane itself. The variation of the ion concentrations in a gradient of the electric potential, i.e., from bulk solution toward the membrane interface, is given by the Boltzmann relations

$$[H^+]_I = [H^+] \exp(-\psi_O F_O/RT) \quad (5a)$$

$$[A^{z+}]_I = [A^{z+}] \exp(-z\psi_O F_O/RT) \quad (5b)$$

$$[HA^{(z+1)+}]_I = [HA^{(z+1)+}] \exp[-(z+1)\psi_O F_O/RT] \quad (5c)$$

Here ψ_O is the membrane surface potential, F_O is the Faraday constant, and RT is the thermal energy. The dissociation reaction of $HA^{(z+1)+}$ is given in bulk solution as

$$[H^+][A^{z+}]/[HA^{(z+1)+}] = K \quad (6a)$$

or in the interfacial region as

$$[H^+]_I[A^{z+}]_I/[HA^{(z+1)+}]_I = K \quad (6b)$$

The fraction of $HA^{(z+1)+}$ in *bulk solution* is

$$f_{HA} = [HA^{(z+1)+}]/([HA^{(z+1)+}] + [A^{z+}]) = (1 + 10^{pH-pK})^{-1} \quad (7a)$$

Correspondingly, the fraction of the protonated species at the *interface* is

$$f_{HA,I} = (1 + 10^{pH_I-pK})^{-1} = (1 + 10^{pH+0.43\psi_O F_O/(RT)-pK})^{-1} \quad (7b)$$

where pH_I is the pH value in the interface. As anticipated, the fraction of $HA^{(z+1)+}$ depends only on the pH at the interface and not on the total charge. The chemical binding step is

Table II: Binding Affinities and in Vitro Activities of a Series of Octapeptide Analogues

somatostatin analogue	el. charge at pH 7.4 ⟨z⟩	receptor binding (pK_i)	relative affinity	inhibition of GH[a] release (pIC_{50})	relative activity	surface[b] conc (nM)
SMS 201-995	1.4	9.4	1.0	8.8	1.00	19.2
SDZ 206-276	1.4	8.6	0.19	8.1	0.17	19.2
SDZ 214-324	2.4	9.6	1.6	8.9	1.10	121
SDZ 217-717	0.4	5.5	0.0002	5.5	0.0004	1.3

[a] GH = growth hormone. [b] Calculated for a bulk concentration of 1 nM peptide, 0.1 M NaCl, and 0.01 Tris buffer pH 7.4, and a membrane composed of POPC/POPG (75/25 mol/mol).

described by a surface partition equilibrium according to

$$X_A = K_1[A^{z+}]_I \quad (8a)$$

$$X_{HA} = K_2[HA^{(z+1)+}]_I \quad (8b)$$

The surface concentrations X_i are defined as the molar amount of species i bound per mole of lipid. In a calorimetric titration experiment, it is not possible to distinguish between the two species A^{z+} and $HA^{(z+1)+}$; only the sum of both species can be measured:

$$X_b = X_A + X_{HA} = K_1[A^{z+}]_I + K_2[HA^{(z+1)+}]_I \quad (9)$$

The relation between X_b and the measured heat of reaction has been discussed previously (Beschiaschvili & Seelig, 1992). The fraction of bound $HA^{(z+1)+}$ relative to the total amount of bound peptide is

$$f_{HA,M} = X_{HA}/(X_{HA} + X_A) = [1 + (K_1/K_2)10^{pH+0.43\psi_O F_O/(RT)-pK}]^{-1} \quad (10)$$

If A^{z+} and $HA^{(z+1)+}$ have the same binding affinity for the membrane ($K_1 = K_2$), eq 10 is identical to eq 7b, i.e., the fractions of the two species A^{z+} and $A^{(z+1)+}$ bound to the membrane are identical to those in the interfacial layer. In contrast, for $K_2 \to \infty$ $f_{HA,M} \to 1$, i.e., only the protonated form binds to the membrane; for $K_2 \to 0$ $f_{AH,M} \to 0$, i.e., only the nonprotonated species if found at the membrane surface. The average peptide charge, defined as

$$\langle z \rangle = (z[A^{z+}] + (z+1)[HA^{(z+1)+}])/([A^{z+}] + [HA^{(z+1)+}]) \quad (11)$$

is calculated at the interfacial layer according to

$$\langle z \rangle = z + f_{AH,I} \quad (12)$$

In the absence of a membrane surface potential ($\psi = 0$) and identical binding constants $K_1 = K_2$, the fraction of $AH^{(z+1)+}$ will be the same in bulk solution, in the interface, and at the membrane surface. In contrast, if the membrane possesses a negative surface potential, the fraction of $AH^{(z+1)+}$ in the interface will be larger than that in the bulk solution ($f_{AH,I} > f_{AH}$). The difference $f_{AH,I} - f_{AH}$ can be calculated from eqs 7a and 7b but can also be determined experimentally as follows. If the binding reaction is measured in buffers of different dissociation enthalpies, the measured reaction enthalpy can be plotted versus the buffer dissociation enthalpy. The slope of the straight line yields the *fraction* of protons, n, associating with or dissociating from the peptide as it binds to the membrane (Beschiaschvili & Seelig, 1992). If $K_1 = K_2$, the calculated difference between bulk solution and interfacial layer, $f_{AH,I} - f_{AH}$, must be identical with the measured uptake or release of protons. However, if $K_1 \neq K_2$ the binding effect will modulate the influence of the surface potential, and from the measured "n" it is possible to evaluate the ratio K_1/K_2 using eqs 10 and 7a.

If X°_{PG} (moles of PG per mole of total lipid) denotes the mole fraction of PG in the membrane and X_{Na} the mole fraction of Na^+ bound to PG, then the surface charge density, σ, can be written as (Beschiaschvili & Seelig, 1990)

$$\sigma = (e_O/A_L)\frac{-X^\circ_{PG}(1 - X_{Na}) + zX_A + (z+1)X_{AH}}{1 + (A_p/A_L)(X_A + X_{AH})} \quad (13)$$

where e_O is the elementary charge, A_L is the surface area of lipid [$A_L = 68$ Å^2 for POPC and POPG (Altenbach & Seelig, 1984; Evans et al., 1987)], and A_p is the surface area requirement of the penetrating peptide ($A_p \simeq 135$ Å^2 for all four peptides).[3] The term $(A_p/A_L)(X_A + X_{AH})$ corrects for the membrane expansion due to peptide penetration (Seelig, 1987; Seelig et al., 1988; Beschiaschvili & Seelig, 1990). Since $(X_A + X_{AH}) < 0.1$ and $A_p/A_L \simeq 2$ in the present study, peptide penetration induces at most a 20% reduction in the membrane surface charge density.

Sodium binding to the PG headgroups follows a Langmuir adsorption isotherm, and a binding constant of $K_{Na} = 0.6$ M^{-1} was used (Eisenberg et al., 1979; Macdonald & Seelig, 1987; Beschiaschvili & Seelig, 1990, 1992).

In addition to eq 9 a second, independent relation between σ and ψ_O is given by the Gouy–Chapman equation [cf. Aveyard and Haydon (1973) and McLaughlin (1977, 1989)]

$$\sigma^2 = 2000\epsilon_O\epsilon_r RT\sum C_{i,eq}(e^{-z_i F_O\psi_O/(RT)} - 1) \quad (14)$$

where $C_{i,eq}$ is the concentration of the ith electrolyte in the bulk aqueous phase (in moles per liter) and z_i is the signed valency of the ith species. The summation is over all ions in solution, including anions. By combining the adsorption/binding equation (eq 13) with the Gouy–Chapman equation (eq 14), a self-consistent solution ψ_O can be found for each experimental value of X_b.

Binding Isotherms. The above model was applied to analyze the calorimetric titration curves. The free parameter in this analysis was the intrinsic binding constant K, characterizing the surface partition equilibrium. All other parameters were provided by independent measurements: (i) The pK of the N-terminal amino group was measured with various methods [potentiometric titrations, surface activity measurements (Seelig, 1990)] and was found to be p$K \sim 7.2$ for all four peptides. The same measurements also showed that the lysine side chains are fully protonated at pH <9.0. The charge parameter, z, was thus identical with the number of lysine residues per molecule. (ii) The reaction enthalpy could be determined independently by injecting a peptide solution into an excess of lipid vesicles under conditions of complete binding [cf. Beshchiaschvili and Seelig (1992)]. The results of these control experiments agreed with the evaluation of ΔH from the reverse lipid → peptide titration experiments.

Figure 3A provides a comparison between the measured (cumulative) heat of reaction and the calculated titration curve for peptide SDZ 214–324. The thermodynamic parameters derived for peptide SDZ 214–324 together with those of the other peptides are summarized in Table I.

Knowledge of K and z allows the calculation of the conventional binding isotherms X_b vs C_{eq}, as shown in Figure 3B for peptide SDZ 214–324. Figure 6A then provides a

[3] For peptide SDZ 217–717 a smaller area of 68 Å^2 should probably be used. These calculations were also performed and yield only minor differences in K.

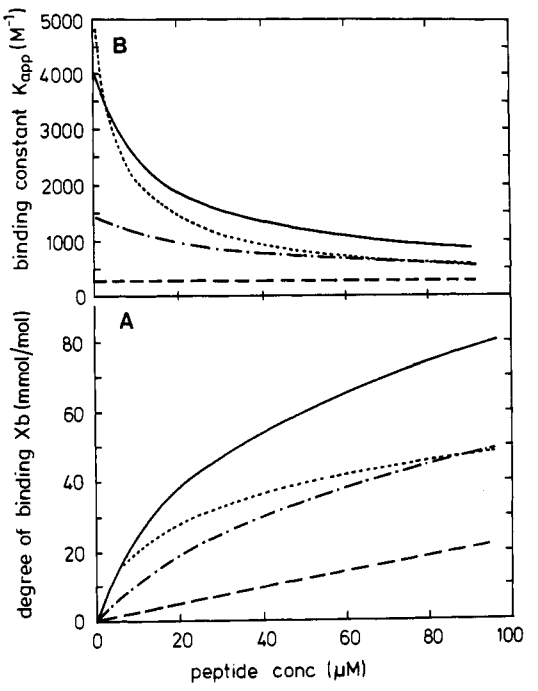

FIGURE 6: Calculated binding isotherms for the different somatostatin analogues based on the experimental parameters deduced from the calorimetric titration experiments. A pK value of 7.2 was assumed for the N-terminal amino group of all four peptides. The calculations refer to pH 7.4, 0.11 M NaCl, and POPC/POPG (75/25 mol/mol) membranes. (A) Variation of the degree of binding, X_b (mmoles of peptide/mole of total lipid), as a function of the free peptide concentration. The following binding constants were used: (–·–) SMS 201–995 with K = 76 M^{-1}; (—) 206–276 with K = 225 M^{-1}; (– – –) SDZ 217–717 with K = 83 M^{-1}; (···) SDZ 214–324 with K = 50 M^{-1}. (B) Variation of the apparent peptide binding constant, $K_{app} = X_b/C_{eq}$, as a function of the peptide concentration. For highly charged peptides, K_{app} is more strongly concentration dependent than for peptides with a small charge.

theoretical comparison of the binding isotherms of all four peptides (pH 7.4, 0.11 M NaCl, vesicles composed of POPC/POPG 75/25 mol/mol, Na^+ binding constant $K_{Na} = 0.6\ M^{-1}$). In the absence of peptide, the membrane surface potential is –48 mV, and the pH at the membrane surface pH 6.6. Figure 6A demonstrates distinct differences in the binding behavior of the four somatostatin analogues. The differences between peptides SMS 201–995, SDZ 217–717, and SDZ 214–324 reflect essentially the influence of the electric charge, since the intrinsic binding constants K are rather similar. The citrullin-containing peptide SDZ 217–717 has the smallest electric charge ($\langle z \rangle$ = +0.4) in solution and exhibits the weakest binding, the Lys^0 containing species SDZ 214–324 with $\langle z \rangle$ = 2.4 exhibits the strongest binding, and species SMS 201–995 with $\langle z \rangle$ = 1.4 is intermediate. For compound SDZ 206–276, which has three aromatic residues on the same face of the peptide ring, the nonpolar interactions increase and the binding isotherm reveals a much larger extent of binding.

From the binding isotherms an *apparent overall binding constant* can be calculated according to

$$K_{app} = X_b/C_{eq} \qquad (15)$$

where C_{eq} is the bulk concentration of peptide in equilibrium with the membrane. The variation of K_{app} with peptide concentration is illustrated in Figure 6B. K_{app} is concentration-independent only for peptide SDZ 217–717 which carries the smallest charge, but K_{app} of this peptide is still a factor of 3 larger than the intrinsic binding constant. For peptide SMS 201–995, K_{app} varies between 1500 M^{-1} at low degrees of binding to about 200 M^{-1} at $C_{eq} \simeq 100\ \mu M$. For peptide SDZ 214–324 with $\langle z \rangle$ = +2.4, the change is even more dramatic with 6000 $M^{-1} > K_{app} > 500\ M^{-1}$.

The lipid binding constants, be it the surface partition constant K or the overall binding constant K_{app}, are small compared to the receptor binding constants, which are usually of the order of $10^9\ M^{-1}$ (dissociation constant $K_D \sim 1$ nM). Nevertheless, lipid binding might still be functionally relevant. Assuming a receptor density of 1 receptor per 1 μm^2 and a lipid-to-protein ratio of 1:1 (wt/wt) for the biological membrane, each receptor molecule is surrounded by about 10^6 lipid molecules. If the lipid binding constant is $K_{app} \sim 200\ M^{-1}$ (e.g., peptide SDZ 217–717), the product "number of lipids × K_{app}" is still less than the receptor binding constant. However, if $K_{app} \sim 5000\ M^{-1}$, as for peptides SDZ 206–276 and SDZ 214–324, the same product is larger than the receptor binding constant. Under these conditions a large percentage of the drug could be bound to the lipid phase and would thus be lost for receptor binding if the receptor site is in the aqueous phase. However, even though the somatostatin receptor has been cloned, the details of its molecular structure are not yet known (Kluxen et al., 1992; Bell & Reisine, 1993).

Membrane-Induced Charge Effects and Peptide Protonation. The electric charges of the peptides are determined by the number of lysine residues per molecule (which are fully protonated at pH ≤7.4) plus the average charge of the N-terminal amino group. The latter can be evaluated using either eq 7a for the bulk solution or eq 7b for the lipid–water interface. The results of such calculations are listed in Table I. The calorimetric titrations can be described with remarkable accuracy using these true physical charges of the peptide molecules which range from $\langle z \rangle$ = +0.4 to $\langle z \rangle$ = +3 (depending on the pH and the location of the peptide). Apparently, the flat ring system of the cyclic peptides together with the small size of the molecules allows all charged residues to come close enough to the interface and to contribute simultaneously to the electrostatic attraction.

As mentioned above, the surface of a negatively charged membrane is more acidic than the bulk solution, leading to an apparent pK shift of the N-terminal amino group [cf. Seelig (1990)]. At a bulk pH of 7.4, the approach to the interfacial layer increases the electric charge of the N-terminal amino group from $\langle z \rangle \simeq 0.38$ (bulk-solution) to $\langle z \rangle \simeq 0.78$ (interfacial layer) (cf. Table I). In contrast, no such effect is predicted at pH 6.25 since the N-terminal amino group (pK ≃ 7.2) is already fully protonated in the buffer phase. Both predictions were verified experimentally by titration calorimetry [cf. Flogel and Biltonen (1975), Biltonen and Langerman (1979), and Morin and Freire (1991) for the detection of protonation reactions with titration calorimetry]. Titration experiments at pH 6.25 in buffers of different dissociation enthalpies yielded a constant reaction enthalpy [cf. Figures 4 and 5; for peptide SMS 201–995, see Beschiaschvili and Seelig (1992), Table II]. No uptake of protons was observed. In contrast, titration experiments at pH 7.4 reveal a linear correlation between the reaction enthalpy, ΔH, and the buffer dissociation enthalpy, ΔH_{Diss} [Figures 4 and 5; eqs 3a and 3b; buffer enthalpies taken from Morin and Freire (1991)]. The measured reaction enthalpy, ΔH, is composed of the intrinsic binding enthalpy, ΔH_1, plus the additional enthalpies of the protonation and deprotonation steps (Beschiaschvili & Seelig, 1992):

$$\Delta H = \Delta H_1 + n(\Delta H_{Diss} - \Delta H_2) \qquad (16)$$

Here ΔH_2 is the dissociation enthalpy of the N-terminal amino

group, while "n" denotes again the *mole fraction* of protons *bound* per mole of peptide. Evaluation of Figures 4 and 5 yields proton fractions of $n = 0.23$ and $n = 0.34$ for peptides SDZ 206–276 and SDZ 217–717, respectively. For peptide SMS 201–995 we have measured previously $n = 0.38$ (Beschiaschvili & Seelig, 1992). The experimentally observed proton uptake is almost identical to (peptide SMS 201–995, SDZ 217–717) or only slightly smaller (peptide SDZ 206–276) than the prediction of the Gouy–Chapman theory with $n = 0.39$ (Table I). The value of 0.23 for SDZ 206–276 can be explained by using eq 10 and assuming $K_1/K_2 \simeq 4$, i.e., the nonprotonated species A^{z+} binds by a factor of 4 better than the protonated species $HA^{(z+1)+}$. As pointed out above, peptide SDZ 206–276 is the most hydrophobic of the peptides investigated since three aromatic residues are lined up on the same side of the peptide ring. It can be speculated that this molecule penetrates deeper into the hydrophobic bilayer than its analogues, favoring deprotonation of the N-terminal amino group.

The intrinsic binding enthalpy, ΔH_1, of the fully protonated peptides follows directly from the ΔH values measured at pH 6.25 and is $\Delta H_1 = -7.0$, -4.7, and -4.5 kcal/mol for peptides SMS 201–995, SDZ 206–276, and SDZ 217–717, respectively. Assuming that these values also hold true for the non-protonated species, combination of eq 16 with the experimental results (eqs 3a and 3b) allows the evaluation of the dissociation enthalpy ΔH_2, yielding $\Delta H_2 = 10.7$, 9.6, and 9.7 kcal/mol for peptides SMS 201–995, SDZ 206–276, and SDZ 217–717, respectively [data for SMS 201–995 were taken from Beschiaschvili and Seelig (1992)]. This result is in good agreement with the dissociation enthalpy of 11 ± 2 kcal/mol of N-terminal amino groups of proteins [cf. Martin (1964) p 79].

Functional Activity and Peptide–Lipid Binding. The somatostatin analogues exert their function by interacting with the active site of the receptor molecule. In the present study, those peptides which revealed a high affinity for the somatostatin receptor were also most effective in inhibiting growth hormone release from pituitary cells. The main effect of the negatively charged membrane is to increase the peptide concentration at the membrane surface. Assuming a peptide bulk concentration of $C_{eq} = 1$ nM, this interfacial concentration can be calculated as $C_I = 3.1$, 19.2, and 121 nM for peptides with average charges of $\langle z \rangle = 0.4$, 1.4, and 2.4 (in solution), respectively. The variation of the surface concentration of the somatostatin analogues parallels (at least qualitatively) the order of binding affinities to the receptor and the functional activities (cf. Table II). SDZ 214–324 ($\langle z \rangle = 2.4$) has the largest surface concentration and thus the highest probability of reaching the active site of the receptor, while SDZ 217–717 ($\langle z \rangle = 0.4$) has the lowest probability. Peptides SMS 201–995 and SDZ 206–276 have the same charge ($\langle z \rangle = 1.4$) and hence accumulate to the same extent at the interface. However, SDZ 206–276 is more hydrophobic and partitions by about a factor of 3 better into the membrane, which can explain the reduced activity of this peptide (by a factor of 5) compared to SMS 201–995, if the active site is only accessible from the aqueous phase.

In summary, the four structurally related cyclic peptides display widely different binding affinities. The experimentally observed electrostatic and nonpolar binding effects on the *lipid* membrane are not sufficient to fully explain the receptor binding affinities. However, the negatively charged membrane surface enhances the binding to the receptor. Penetration into the hydrophobic part of the membrane appears to be functionally unfavorable.

ACKNOWLEDGMENT

We thank Dr. Anna Seelig and Ms. Sandra Lotz for monolayer measurements of SMS 201–995 and SDZ 217–717 and for valuable discussions.

REFERENCES

Altenbach, Ch., & Seelig, J. (1984) *Biochemistry 23*, 3913–3920.
Aveyard, R., & Haydon, D. A. (1973) *An Introduction to the Principles of Surface Chemistry*, Cambridge University Press, London.
Bell, G. I., & Reisine, T. (1993) *Trends Neurosci. 16*, 34–38.
Beschiaschvili, G., & Seelig, J. (1990) *Biochemistry 29*, 10995–11000.
Beschiaschvili, G., & Seelig, J. (1991) *Biochim. Biophys. Acta 1061*, 78–84.
Beschiaschvili, G., & Seelig, J. (1992) *Biochemistry 31*, 10044–10053.
Biltonen, R. L., & Langerman, N. (1979) *Methods Enzymol. 61*, 287–318.
Bruns, Ch., Dietl, M., Palacios, J. M., & Pless, J. (1990) *Biochem. J. 265*, 39–44.
Cantor, C. R., & Schimmel, P. R. (1980) *Biophysical Chemistry*, Vol. I, p 283, Freeman, San Francisco, CA.
Cevc, G., & Marsh, D. (1987) *Phospholipid Bilayers. Physical Principles and Models*, Wiley-Interscience, New York.
De Lean, A. (1979) Ph.D. Thesis, Duke University, NC.
Eisenberg, M., Gresalfi, T., Riccio, T., & McLaughlin, S. (1979) *Biochemistry 18*, 5213–5223.
Evans, R. W., Williams, M. A., & Tinoco, J. (1987) *Biochem. J. 245*, 455–462.
Fernandez, M. S., & Fromherz, P. (1977) *J. Phys. Chem. 81*, 1755–1761.
Flogel, M., & Biltonen, R. L. (1975) *Biochemistry 14*, 2610–2615.
Fromherz, P. (1975) *Rev. Sci. Instrum. 46*, 1380–1385.
Fromherz, P. (1989) *Methods Enzymol. 171*, 376–387.
Herbette, L. G., Rhodes, D. G., & Mason, R. P. (1991) *Drug Des. Delivery 7*, 75–118.
Holladay, L., Rivier, J., & Puett, D. (1977) *Biochemistry 16*, 4895–4900.
Kluxen, F. W., Bruns, Ch., & Lübbert, H. (1992) *Proc. Natl. Acad. Sci. U.S.A. 89*, 4618–4622.
Macdonald, P. M., & Seelig, J. (1987) *Biochemistry 26*, 1231–1240.
Martin, B. R. (1964) Introduction to Biophysical Chemistry, McGraw-Hill, New York.
Maurer, R., Gaehwiler, B. H., Buescher, H. H., Hill, R. C., & Roemer, D. (1982) *Proc. Natl. Acad. Sci. U.S.A. 79*, 4815–4817.
McLaughlin, S. A. (1977) *Curr. Top. Membr. Transp. 9*, 71–144.
McLaughlin, S. (1989) *Annu. Rev. Biophys. Biophys. Chem. 18*, 113–136.
Miyazaki, J., Hideg, K., & Marsh, D. (1992) *Biochim. Biophys. Acta 1103*, 62–68.
Morin, E. P., & Freire, E. (1991) *Biochemistry 30*, 8494–8500.
Mosior, M., & McLaughlin, S. (1992) *Biochemistry 91*, 1767–1773.
Reubi, J. C., Perrin, M. H., Rivier, J. E., & Vale, W. (1981) *Life Sci. 28*, 2191–2198.
Rhodes, D. G., Sarmiento, J. G., & Herbette, L. G. (1985) *Mol. Pharmacol. 27*, 612–623.
Schwyzer, R. (1987) *EMBO J. 6*, 2255–2259.
Seelig, A. (1990) *Biochim. Biophys. Acta 1030*, 111–118.
Seelig, A. (1992) *Biochemistry 31*, 2897–2904.
Vale, W., & Grant, G. (1975) *Methods Enzymol. 37*, 82–93.
Wiseman, T., Willigston, S., Brandts, J. F., & Lung-Nau, L. (1989) *Anal. Biochem. 179*, 131–137.